

Syntheses, Characterization of Graphite Nanoparticles and Reduced Graphite Oxide Nanoparticles Derived from Wheat Straw

Ban D. Saleh 1, Ghazwan H. Abdulwahhab2, Safaa M. Rashid3

1Chemistry Department - College of Education for Women - Tikrit University. Salah Al-Din - Iraq.

2Chemistry Department - College of Education for Pure Sciences - Tikrit University. Salah Al-Din - Iraq

3Department of Chemical Engineering- College of Engineering- Tikrit University. Salah Al-Din - Iraq

E-mail: baan.saleh@tu.edu.iq

Abstract:

In this study, wheat straw graphite WSGt: B2 was prepared by burning ground straw in an oven at (30-700) °C. Then WSRGO: B4 reduced graphene oxide was prepared by microwave by reducing the prepared carbon nanotube by Hummer method by adding an appropriate amount of it in a ceramic jar, then inserting it into the microwave at a temperature of 500 °C for 3 minutes. The prepared nanocomposites were diagnosed by physical processes such as melting point as well as spectroscopic methods such as Infrared Spectra (FT-IR), Atomic Force Microscopy (AFM), Scanning Electron Microscopy (SEM) and diffraction X-ray. According to the findings, there are visible variances in the number of layers in nanoparticles. A low value indicates the existence of cavities inside the nanoparticles. The number of layers between nanocomposites increases. It was discovered that the link between the grain size peaks D and the number of layers and the distances between them is not necessarily straightforward. This is due to differences in the additive compositions on the plates.

Keywords: Nanoparticles, Graphene oxide nanoparticles, Wheat straw, Hummer method.

توليف وتوصيف جزيئات الجرافيت النانوية وجزيئات نانوية منخفضة من أكسيد الجرافيت المشتقة من قش القمح

بان داوود صالح 1 ، غزوان عبدالوهاب2 ، صفاء محمد راشد3

1 قسم الكيمياء - كلية التربية للبنات - جامعة تكريت. صلاح الدين - العراق.

2 قسم الكيمياء - كلية التربية للعلوم الصرفة - جامعة تكريت. صلاح الدين - العراق.

3 قسم الهندسة الكيميائية. كلية الهندسة - جامعة تكريت. صلاح الدين - العراق.

الخلاصة:

في هذه الدراسة تم تحضير جرافيت قش القمح WSGt: B2 بحرق قش مطحون في فرن عند (30-700) درجة مئوية. بعد ذلك تم تحضير WSRGO: B4 أكسيد الجرافين المختزل بواسطة الميكروويف عن طريق تقليل أنبوب الكربون النانوي المحضر بطريقة هامر عن طريق إضافة كمية مناسبة منه في وعاء خزفي ، ثم إدخاله في الميكروويف عند درجة حرارة 500 درجة مئوية ولمدة 3 دقائق. تم تشخيص المركبات النانوية المحضرة من خلال العمليات الفيزيائية مثل نقطة الانصهار وكذلك طرق التحليل الطيفي مثل أطيف الأشعة تحت الحمراء FT-IR ، مجهر القوة الذرية AFM ، الفحص المجهر الإلكتروني SEM وكذلك الحيويد بالأشعة السينية. وفقاً للنتائج ، هناك اختلافات واضحة في عدد طبقات الجسيمات النانوية. تشير القيمة المنخفضة إلى وجود تجاويف داخل الجسيمات النانوية. يزداد عدد الطبقات بين المركبات النانوية. تم اكتشاف أن الارتباط بين حجم الجسيمات D وعدد الطبقات والمسافات بينها ليس بالضرورة مباشراً. هذا بسبب الاختلافات في التراكيب المضافة على اللوحات. الكلمات المفتاحية: الجسيمات النانوية ، الجسيمات النانوية من أكسيد الجرافين ، قش القمح ، طريقة هامر.

1. Introduction

Wheat straw is the finest bioethanol, biogas, and bio-hydrogen feedstock for bio refineries since it is renewable, widely dispersed, and inexpensive [1]. It is ecologically friendly and safe to consume. It is a low-cost substrate and a natural source of biofuels, and it contains anti-inflammatory, antibacterial, anti-arterial, anti-allergic, antioxidant, and anticoagulant properties. Nanomaterials are split into two categories [2]. One is from top to bottom, in which the initial (extensive) substance is gradually broken down until it reaches the nanoscale [3]. Light drilling, cutting, grinding, and fragmentation are utilized to accomplish this [4]. Two-dimensional flat sheets of graphite [5]. These sheets have a thickness of one carbon atom in diameter. The graphene form (sp^2) represents the hybridization process between carbon atoms [6]. In the case of graphene oxide, the hybridization between carbon atoms is in the state (sp^3), which involves attaching each carbon atom to four nearby carbon atoms to create a tetrahedral vertex [7]. In the case of the arrangement (sp^2), each carbon atom has three carbon atoms adjacent to it [8]. Thus, it will be a geometrical shape of six atoms linked, forming a ring. All plates have this hybridization (sp^2). Because nanographene has the feature of electrical conductivity [9], other nanographene of different sorts has double bonds in specific bonding locations. It is dubbed super car-

bon because it has a high conductivity relative to all other nanomaterials and non-nano materials, which is even more significant than the conductivity of metals. It also has high optical transparency [10]. It's a thick carbon-based atomic sheet with hexagonal lattice sheets. The extensive use of graphene favors its high area, chemical stability, and electrical qualities [11]. Carbon-based graphene is renowned as the lightest and most powerful of materials. As a result, graphene possesses remarkable physical, chemical, mechanical, thermal, and optical characteristics, opening up many uses [12]. The graphene oxide is made from graphene, and the approach is an ecologically friendly modification of the Hummer process. Graphene, not graphite particles, is the carbon source. Many safety and health issues are alleviated by toxic gases such as NO_2/N_2O_4 [13]. As a result, as compared to traditional approaches, the response time is lowered [14]. Because graphene has a greater surface area per volume, the oxidized groups are spread quickly and uniformly over the graphene network, reducing the need for further sonication procedures to separate the layers [15].

2. Procedure

2.1. Chemicals used:

All chemicals used in this work were purchased from BDH, Aldrich and Fluka companies and were used without further purification.

2.2. Devices used:

The FT-IR spectra were captured using a Shimadzu FT-IR 8400S spectrophotometer with a (400-4000) cm^{-1} by KBr disc. (AFM) Atomic Force Microscopy Use the device (AFM icon. Bruke Q600 US) at Kashan University- Iran. Scanning Electron Microscopy (SEM) device (Czech Republic/ Belsorp Mini II/ TE SCAN) was used at Kashan University - Iran. X-ray diffraction device Using (Shimadzu-XRD-6000) Kashan University- Iran. Microwave oven rated voltage AC220-2240 and rated frequency 50Hz

2.3. Methods for The Preparation of Nanoparticles

2.3.1. Preparation of wheat straw kraft WSGt: B2 [16,17]:

The preparation process included two steps:

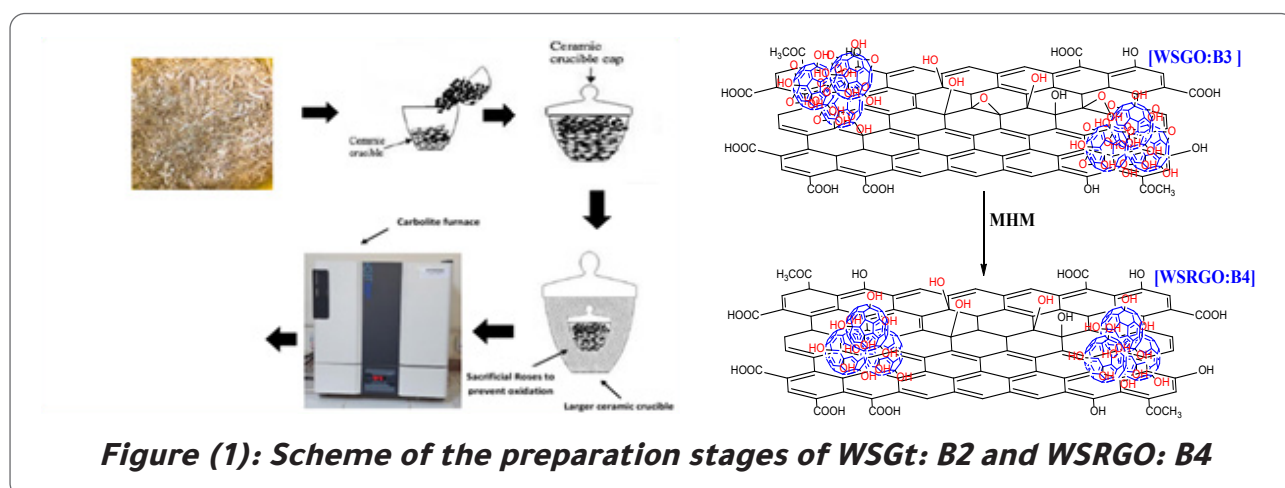
First: The process of preparing the Wheat Straw WSt: B1: 1 gm of wheat stalks were collected and washed several times (3x50 ml distilled water) to remove silica (dust) and other suspended contaminants, then dried in the shade, at a temperature 35 °C, and

until the weight was stable, then it was ground and used for the study, and this step was repeated several times until a sufficient quantity was formed for all subsequent experiments.

Second: Preparation of wheat straw graphite WSGt: B2: I put an appropriate amount of crushed wheat straw stalks in a small ceramic pot and put the pulp in the middle of a larger ceramic pot. I filled the space between the two puddings with a sufficient amount of graphite flour, which was plasticized (heated) to the point of combustion) in a burning furnace at a gradual rising temperature from (30-700) °C for one (1) hour, as shown in figure (1).

2.3.2. Microwave preparation of reduced graphene oxide WSRGO: B4 [18, 19]:

Hummer WSGO reduced the prepared Nano carbon: B3 method by adding an appropriate amount of it in a ceramic jar and then inserted into the microwave at a temperature of 500 °C for 3 minutes, and rated power input for 1150w and rated power output for 700w.



3. Results and Discussion:

3.1. Discussion of the compound

WSGt: B2:

Wheat straw graphite WSGt: B2 was prepared by burning an appropriate amount of straw flour WS: B1 in an earthen pot at (30-700) °C for one hour, where the plates are formed through the following

suggested mechanism in figure (2). When studying the infrared (IR) spectrum of the prepared compound [WSGt: B2], it was observed that a band appeared at a frequency (3321) cm^{-1} belonging to the alcoholic (OH) group. Absorption bands appeared at the frequency (3020) cm^{-1} due to the stretching of the aromatic (CH) bond. The appearance of two rounds at the frequency (2958, 2885) cm^{-1} belonging to the aliphatic (CH) group, as well as the appearance of an absorption band at the frequency (1718) cm^{-1} is due to the stretching of the carbonyl (C=O) ketogenic bond, and the appearance of two absorption bands at the frequency (1593, 1494) cm^{-1} due to the stretching of the aromatic (C=C) bond, and the appearance of an absorption band at the frequency (1367-1100) cm^{-1} belongs to a group (C-O), as shown in figure (3), as these bundles were close to what is found in the literature [20-24].

The X-ray spectrum of the compound (WSGT: B2) showed an angle value of 2θ at 28.3867 with interlayer

distances $d=3.14418$, with a grain size of $D=24.86$ and several layers

$n=7.90667$. It was noted that these values are close to the literature [25, 26]. It is indicated in figure (3).

From the morphological FESEM images of the sample WSGt: B2, it was observed that there were larger

cracks compared to WS: B1. With apparent gaps remaining b with a nano-thickness of the sheet c with

spherical structures of different sizes on the surfaced [27-30], as in figure (4).

Atomic force microscopy (AFM) images of the surface of the WSGt: B2 material showed the presence of

apparent cracks in the plate a, some blunt elevations on the surface of the plate b with longitudinal

regularity of the formed plates c with the formation of divergent vessels with heights up to 890 nm d,

and all the properties were close to the SEM images above [31], as in figure (5).

3.2. Discussion of the compound

WSRGO: B4:

Compound WSRGO: B4 was prepared from WSGO: B3 reduction by microwave irradiation: MWI at 500°C for 3 minutes. The associated reduced graphene oxide (WSGO: B3), accompanied by the orbital hybridization of carbon from sp^3 to sp^2 , has been reduced. (O = 0%) for graphene oxide (WSGO: B3) in most cases, so reduced graphene oxide (WSRGO: B4) is defined as the reducing derivative of (WSGO: B3) [32] shown in figure (2).

When studying the infrared (IR) spectrum of the prepared compound

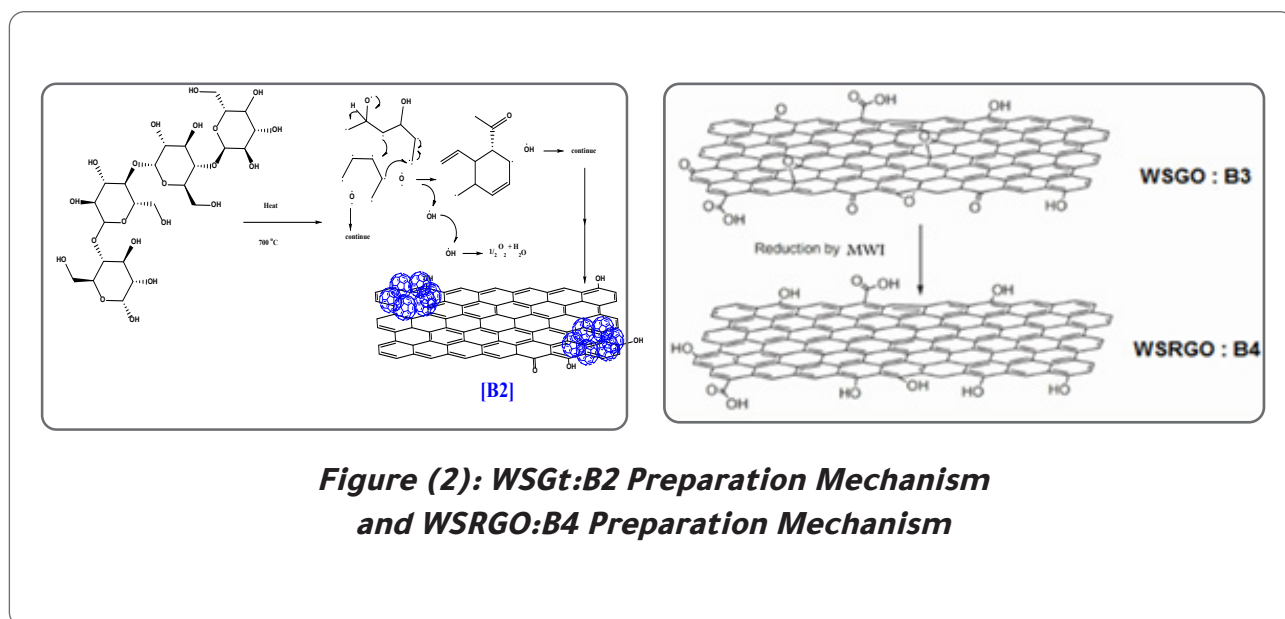
[WSRGO:B4], it was observed that a beam appeared at a frequency (3396) cm^{-1} belonging to the (OH) group, and a beam occurred at a frequency (3058) cm^{-1} belonging to the aromatic (CH) group, and the appearance of two bands at frequency (2941, 2846) cm^{-1} belonging to the aliphatic (CH) group, and the appearance of an absorption band at a frequency (1720) cm^{-1} belonging to the carbonyl group (C=O) carboxylic, with the appearance of two absorption bands at the frequency (1589, 1498) cm^{-1} due to the stretching of the aromatic (C=C) bond, as shown in figure (6), and these were the packages are similar to what is found in the literature [33,34].

The X-ray spectrum of the compound (WSRGO: B4) showed an angle value of 2θ at 23.37 with interlayer distances $d=3.80357$, a grain size of $D=1.09$, and several layers $n= 0.28657$.

It was noted that these values are close to the literature [35], notes figure (6).

From the morphological FESEM images of the sample WSRGO: B4, two phenomena were observed, the first being the high flat equatorial surface of the a1-5 plates, with surface cracks remaining to a lesser degree compared to in B3, spherical particles are collected on the surface to give another type of carbon, which is fullerene, in a polymerized form on the surfaces of the plates b1-5, c with regular holes of close diameters $d_{1,2}$ [36], notes figure (7).

The surface was studied using AFM of the compound WSRGO: B4, and the images showed chains of peaks a1-4 with gaps adjacent to cracks a5-8 and peaks heights of up to 35 nm b, c with The appearance of equatorial d indicates the heterogeneity of the sample [37], it is noted in figure (8).



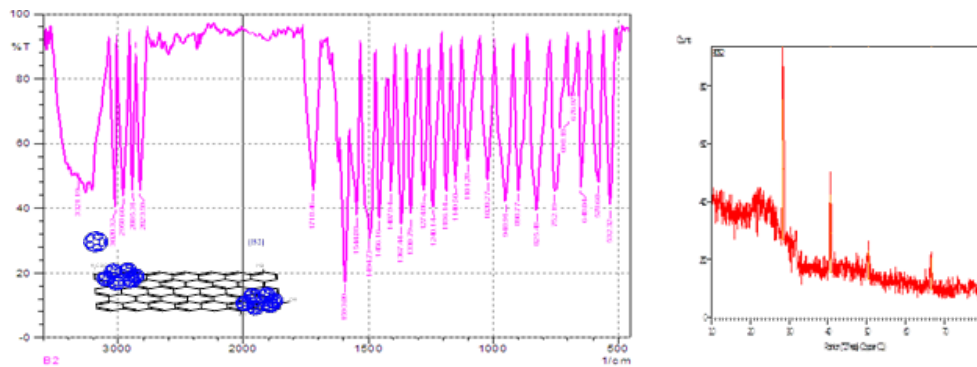


Figure (3): Infrared and X-ray spectrum of the matrix (WSGt: B2)

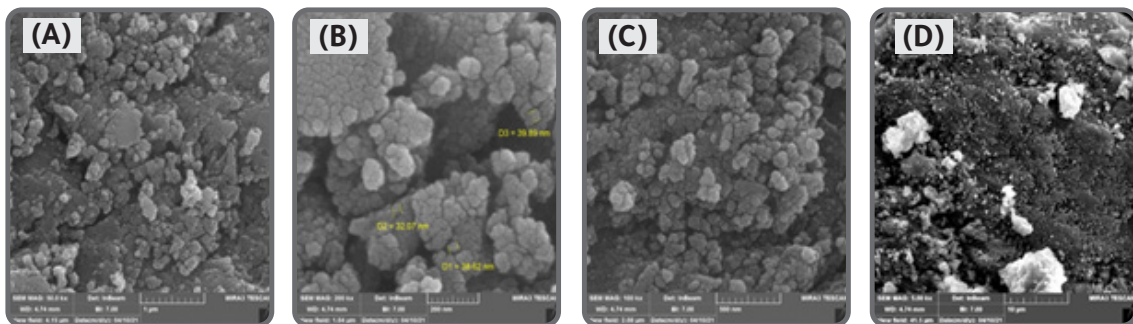


Figure (4): FESEM images of the matrix (WSGt: B2)

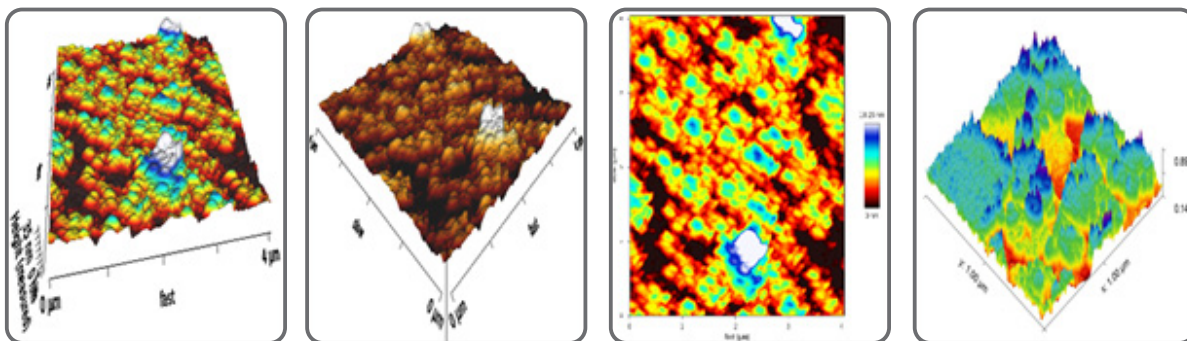


Figure (5): AFM images of the matrix (WSGt: B2)

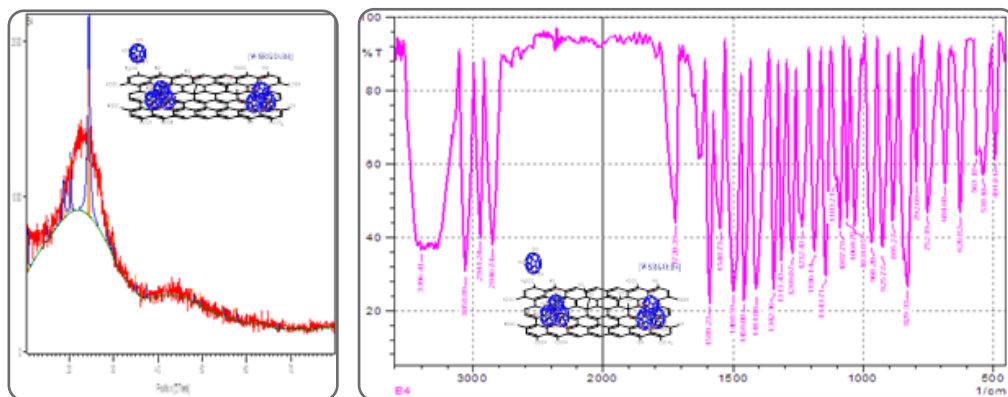


Figure (6): Infrared and X-ray spectrum of the matrix (WSRGO: B4)

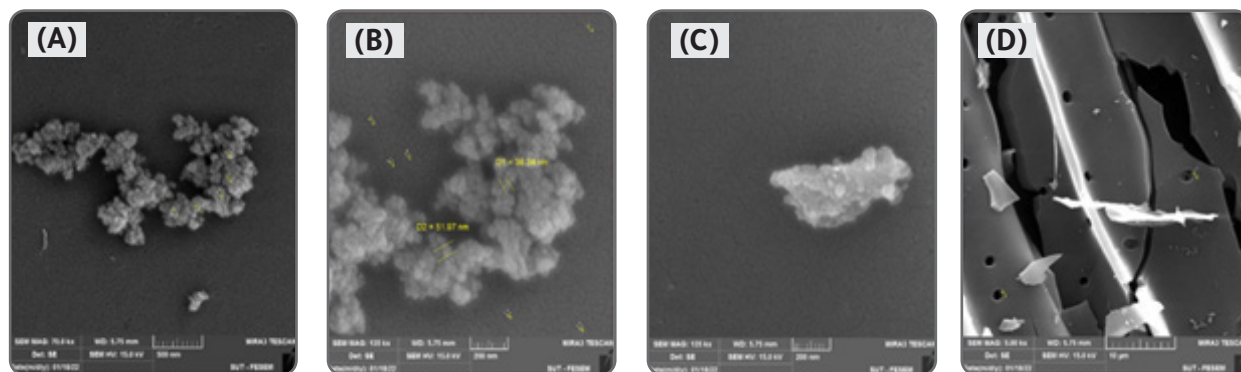


Figure (7): FESEM images of the matrix (WSRGO: B4)

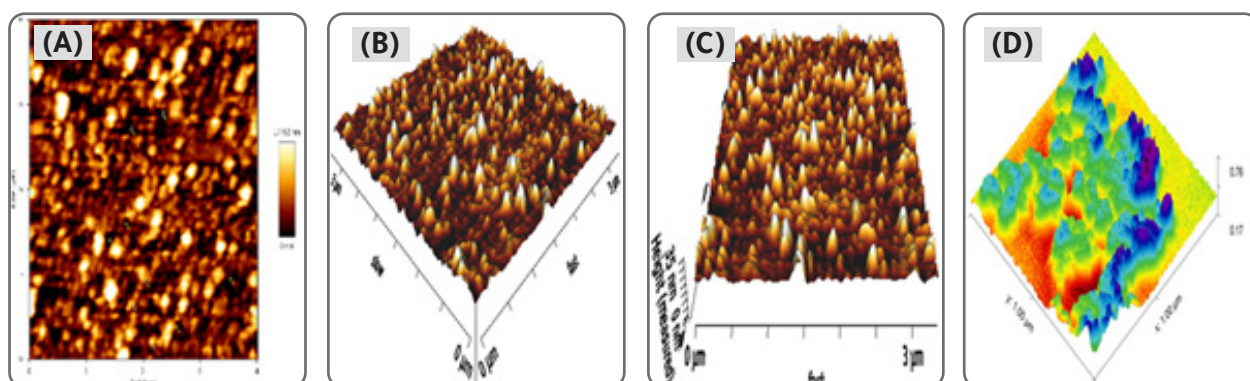


Figure (8): AFM images of the matrix (WSRGO: B4)

Conclusions: The physical and spectroscopic measurements proved and confirmed the validity and accuracy of the structures of the prepared nanocomposites. Graphene oxide can be prepared by using the Hammer method. The increase in the number of layers is due to the different composition of each plate, as it does not have similar degrees of oxidation, which leads to the convergence of the leaves and an increase in their number. In contrast, the number began to decrease with the presence of decoration. The relationship is not always direct be-

tween the grain size peaks d and the number of layers nor the distances between them d , which is due to the difference in the composition of the materials added to the plates. Effective nanocomposites can be prepared in both applied and medical fields. The associated reduced graphene oxide (WSGO: B3), accompanied by the orbital hybridization of carbon from sp^3 to sp^2 , has been reduced. ($O=0\%$) for graphene oxide (WSGO: B3) in most cases, so reduced graphene oxide (WSRGO: B4) is defined as the reducing derivative of (WSGO: B3).

References

- 1- Edelstein, A. S., & Cammaratra, R. C. (Eds.). (1998). *Nanomaterials: synthesis, properties and applications*. CRC press.
- 2- Buchspies, B., Kaltschmitt, M., & Junginger, M. (2020). Straw utilization for biofuel production: A consequential assessment of greenhouse gas emissions from bioethanol and biomethane provision with a focus on the time dependency of emissions. *GCB Bioenergy*, 12(10), 789-805.
- 3- Branska, B., Fořtová, L., Dvořáková, M., Liu, H., Patakova, P., Zhang, J., & Melzoch, M. (2020). Chicken feather and wheat straw hydrolysate for direct utilization in biobutanol production. *Renewable Energy*, 145, 1941-1948.
- 4- Zhu, Y., Murali, S., Cai, W., Li, X., Suk, J. W., Potts, J. R., & Ruoff, R. S. (2010). Graphene and graphene oxide: synthesis, properties, and applications. *Advanced materials*, 22(35), 3906-3924.
- 5- Wang, H., Yuan, X., Wu, Y., Huang, H., Peng, X., Zeng, G., & Ren, M. (2013). Graphene-based materials: fabrication, characterization and application for the decontamination of wastewater and wastegas and hydrogen storage/generation. *Advances in Colloid and Interface Science*, 195, 19-40.
- 6- Fedirko, V. A. (2014). Electron Tunneling from Graphene.
- 7- Savage, N. (2012). Materials science: Super carbon. *Nature*, 483(7389), S30-S31.
- 8- Nair, R. R., Blake, P., Grigorenko, A. N., Novoselov, K. S., Booth, T. J., Stauber, T., & Geim, A. K. (2008). Fine structure constant defines visual transparency of graphene. *Science*, 320(5881), 1308-1308.
- 9- Geim, A. K. (2009). Graphene: status and prospects. *science*, 324(5934), 1530-1534.
- 10- De Silva, K. K. H., Huang, H. H., Joshi, R. K., & Yoshimura, M. (2017). Chemical reduction of graphene oxide using green reductants. *Carbon*, 119, 190-199.
- 11- Thakur, S., & Karak, N. (2015). Alternative methods and nature-based reagents for the reduction of graphene oxide: A review. *Carbon*, 94, 224-242.
- 12- Costa, M. C., Marangoni, V. S., Ng, P. R., Nguyen, H. T., Carvalho, A., & Castro Neto, A. H. (2021). Accelerated Synthesis of Graphene Oxide from Graphene. *Nanomaterials*, 11(2), 551.
- 13- Liu, Z., Zheng, Q. S., & Liu, J. Z. (2010). Stripe/kink microstructures formed in mechanical peeling of highly orientated pyrolytic graphite. *Applied Physics Letters*, 96(20), 201909.
- 14- Wang, D., Vijapur, S. H., & Botte, G. G. (2014, September). Coal char derived few-layer graphene anodes for lithium ion batteries. In *Photonics* (Vol. 1, No. 3, pp. 251-259). Multidisciplinary Digital Publishing Institute.
- 15- Boyd, J. (2006). Rice Chemists Create, Grow Nanotube Seeds Used to Sprout Nanotubes. *Rice News*, 30.
- 16- Hata, K., Futaba, D. N., Mizuno, K., Namai, T., Yumura, N., & Iijima, S. (2006). NIR photoluminescence and resonant raman mappings of SWNT.

Science, 306, 1362-5.

17- Chua, C. K., & Pumera, M. (2014). Chemical reduction of graphene oxide: a synthetic chemistry viewpoint. *Chemical Society Reviews*, 43(1), 291-312.

18- Futaba, D. N., Hata, K., Yamada, T., Mizuno, K., Yumura, M., & Iijima, S. (2005). Kinetics of water-assisted single-walled carbon nanotube synthesis revealed by a time-evolution analysis. *Physical review letters*, 95(5), 056104.

19- Hiraoka, T., Izadi Najafabadi, A., Yamada, T., Futaba, D. N., Yasuda, S., Tanaike, O., & Hata, K. (2010). Compact and light supercapacitor electrodes from a surface-only solid by opened carbon nanotubes with 2 200 m² g⁻¹ surface area. *Advanced Functional Materials*, 20(3), 422-428.

20- Zhang, X., An, Y., Han, J., Han, W., Zhao, G., & Jin, X. (2015). Graphene nanosheet reinforced ZrB₂-SiC ceramic composite by thermal reduction of graphene oxide. *Rsc Advances*, 5(58), 47060-47065.

21- Abd, I. Q., Ibrahim, H. I., Jirjes, H. M., & Dalaf, A. H. (2020). Synthesis and Identification of new compounds have Antioxidant Activity Beta-carotene, from Natural Auxin Phenyl Acetic Acid. *Research Journal of Pharmacy and Technology*, 13(1): 40-46.

22- Jabar, S. A., Hussein, A. L., Dalaf, A. H., & Aboud, H. S. (2020). Synthesis and Characterization of Azetidine and Oxazepine Compounds Using Ethyl-4-((4-Bromo Benzylidene) Amino) Benzoate as Precursor and Evaluation of Their Biological Activity. *Journal of Ed-*

ucation and Scientific Studies, 5(16).

23- Dalaf, A. H. (2018). Synthesis and Characterization of Some Quartet and Quinary Heterocyclic Rings Compounds by Traditional Method and Microwave Routes Method and Evaluation of Their Biological Activity. M.Sc. Thesis, Tikrit University, Tikrit, Iraq: 1-94 pp.

24- Dalaf, A. H., & Jumaa, F. H. (2018). Synthesis, Characterization of some 1,3-Oxazepane -4,7-Dione by Traditional and Microwave routes method and evaluation of their biological activity. *Al-utroha for Pure Science*. (8): 93-108.

25- Dalaf, A. H., Jumaa, F. H., & Jabbar, S. A. S. (2018). Synthesis and Characterization of some 2, 3-dihydroquinoline and evaluation of their biological activity. *Tikrit Journal of Pure Science*, 23(8): 66-67.

26- Salwa, A. J., Ali, L. H., Adil, H. D., Hossam, S. A. (2020). Synthesis and Characterization of Azetidine and Oxazepine Compounds Using Ethyl-4-((4-Bromo Benzylidene) Amino) Benzoate as Precursor and Evaluation of Their Biological Activity. *Journal of Education and Scientific Studies*, ISSN: 24134732. 16(5): 39-52.

27- Dalaf, A. H., & Jumaa, F. H. (2020). Synthesis, Identification and Assess the Biological and Laser Efficacy of New Compounds of Azetidine Derived from Benzidine. *Muthanna Journal of Pure Science (MJPS)*, 7(2):12-25.

28- Saleh, R. H., Rashid, W. M., Dalaf, A. H., Al-Badrany, K. A., & Mohammed, O. A. (2020). Synthesis of Some New

Thiazolidinone Compounds Derived from Schiff Bases Compounds and Evaluation of Their Laser and Biological Efficacy. *Ann Trop & Public Health*, 23(7): 1012-1031.

29-Yass, I. A., Aftan, M. M., Dalaf, A. H., & Jumaa, F. H. (Nov. 2020). Synthesis and Identification of New Derivatives of Bis-1,3-Oxazepene and 1,3-Diazepine and Assess the Biological and Laser Efficacy for Them. The Second International & The Fourth Scientific Conference of College of Science - Tikrit University. (P4): 77-87.

30- Salih, B. D., Dalaf, A. H., Alheety, M. A., Rashed, W. M., & Abdullah, I. Q. (2021). Biological activity and laser efficacy of new Co (II), Ni (II), Cu (II), Mn (II) and Zn (II) complexes with phthalic anhydride. *Materials Today: Proceedings*, 43, 869-874.

31-Aftan, M. M., Jabbar, M. Q., Dalaf, A. H., & Salih, H. K. (2021). Application of biological activity of oxazepine and 2-azetidinone compounds and study of their liquid crystalline behavior. *Materials Today: Proceedings*, 43, 2040-2050.

32-Aftan, M. M., Talloh, A. A., Dalaf, A. H., & Salih, H. K. (2021). Impact para position on rho value and rate constant and study of liquid crystalline behavior of azo compounds. *Materials Today: Proceedings*.

33-Aftan, M. M., Toma, M. A., Dalaf, A. H., Abdullah, E. Q., & Salih, H. K. (2021). Synthesis and Characterization of New Azo Dyes Based on Thiazole and Assess the Biological and Laser Efficacy for Them and Study their Dyeing Applica-

tion. *Egyptian Journal of Chemistry*, 64(6), 2903-2911.

34- Khalaf, S. D., Ahmed, N. A. A. S., & Dalaf, A. H. (2021). Synthesis, characterization and biological evaluation (antifungal and antibacterial) of new derivatives of indole, benzotriazole and thioacetyl chloride. *Materials Today: Proceedings*.6201- ,(17)47 6210.

35-Dalaf, A. H., Jumaa, F. H., & Salih, H. K. (2021). Preparation, Characterization, Biological Evaluation and Assess Laser Efficacy for New Derivatives of Imidazolidin-4-one. *International Research Journal of Multidisciplinary Technovation*, 3(4), 41-51.

36-Dalaf, A. H., Jumaa, F. H., & Salih, H. K. (2021). MULTIDISCIPLINARY TECHNOLOGICAL RESEARCH. *Red*, 15(A2), C44H36N10O8.

37-Dalaf, A. H., Jumaa, F. H., Aftana, M. M., Salih, H. K., & Abd, I. Q. (2022). Synthesis, Characterization, Biological Evaluation, and Assessment Laser Efficacy for New Derivatives of Tetrazole. In *Key Engineering Materials* (Vol. 911, pp. 33-39). Trans Tech Publications Ltd.